

# SELECTIVE OSTEOBLASTIC CELL MICRO-ARRAYS ON DIAMOND FILMS

Bohuslav Rezek, Lenka Michalíková, Egor Ukraintsev, Alexander Kromka

*Institute of Physics, Academy of Sciences of the Czech Republic, Cukrovarnicka 10, Prague 6, Czech Republic*

Marie Kalbacova

*Institute of Inherited Metabolic Disorders, 1st Faculty of Medicine, UK, Ke Karlovu 2, Prague 2, Czech Republic*

**Keywords:** Cell adhesion, Proteins, Diamond, Biotechnology, Biosensors, Osteoblasts, Atomic force microscopy.

**Abstract:** Unique combination of chemical and biocompatible properties with semiconducting properties makes diamond an attractive material for merging solid state and biological systems. Microscopic chemical patterning of diamond films by hydrogen and oxygen surface atoms is used for self-assembly of human osteoblastic cells into micro-arrays. The cell adhesion and assembly on the diamond is further controlled and optimized by cell and protein (fetal bovine serum - FBS) concentration. The cells are characterized by fluorescence microscopy of actin fibers and nuclei. The protein adsorption is studied by atomic force microscopy (AFM). The cells are arranged into arrays on O-terminated patterns. The best cell selectivity is achieved for the lowest cell concentrations of 2500 cells/cm<sup>2</sup>. Higher cell concentrations enable to colonize unfavorable H-terminated regions due to mutual cell communication. Based on AFM, the proteins are present on both H- and O-terminated surfaces, however, pronounced differences in the thickness, surface roughness, morphology, and phase images indicate different conformation of the proteins and hence the cell selectivity. There is no cell selectivity when no protein is supplemented in the medium. These results may be applicable in tissue engineering, implants, bio-electronics, and biotechnology in general.

## 1 INTRODUCTION

Diamond is not only a gem but also a promising technological material. Its properties include high hardness, fracture toughness, low friction coefficient, high Young modulus, increased wear resistance and a variety of substrates onto which it can be prepared (Potocky, 2007). Although diamond is considered inert, its surface can be functionalized by various atoms or molecules (Rezek, 2007a). This gives rise to striking properties (Nebel, 2003).

For instance, electrical conductivity and electron affinity of diamond are strongly influenced by the O- or H-termination of the diamond surface (Kawarada, 1996; Maier, 2001). The differences are mainly caused by the surface dipole of C-H and C-O bonds (Tachiki, 2003). O-terminated diamond is highly resistive, whereas H-terminated surface induces p-type surface conductivity even on an undoped diamond (Maier, 2001). These features can

be applied for field-effect transistor (FET) devices (Rezek, 2007b; Garrido, 2003).

Furthermore, O-terminated surfaces are hydrophilic while H-terminated surfaces are hydrophobic. H-terminated surfaces were thus found less favorable for osteoblastic cell adhesion, spreading and viability compared to O-terminated surfaces (Kalbacova, 2007a). On the other hand, H-terminated diamond surface is an ideal starting point for covalent attachment of biomolecules (Yang, 2002). Chemical functionalization can also lead to bio-passivation or bio-active properties (Bajaj, 2007).

Unique combination of the mechanical, chemical, and biocompatible properties (Tang, 1995, Kalbacova, 2007a) with semiconducting properties makes diamond an attractive material for merging solid state and biological systems (Yang, 2004; Rezek, 2007b). Hence the hydrogen and oxygen surface patterns are highly relevant for bio-electronics as well as for tissue engineering.

Characterization of the interaction between cells and surfaces is essential for cell-based biosensors, engineered tissue therapies and the optimization of implant biomaterials. Cells recognize their environment and consequently start to change it by a production of appropriate extracellular matrix (ECM) proteins to form the basis for cell spreading, increased adhesion and expression of differentiated phenotypes (Schakenraad, 1989). This complex and flexible process is dependent on culture conditions, including the underlying substrate and the pre-adsorbed protein layer.

Until now, the research on the cell-diamond interfaces has been focused on overall homogeneous surface terminations (Yang, 2004; Kalbacova, 2007a; Rezek, 2007c; Song, 2007). In this work we show selective adhesion and arrangement of osteoblast-like cells on NCD thin films that are microscopically patterned with H- and O-terminated regions (Michalikova, 2008). We control initial cell density and serum concentration in medium influencing cellular colonization of patterned substrate. Furthermore, we employ atomic force microscopy (AFM) to characterize the structural properties of mediating proteins (fetal bovine serum, a crucial component for the cell growth) adsorbed onto the diamond micro-patterns. The data are used to discuss the selectivity of the cell adsorption on the patterns, i.e. to what degree the cell adhesion and its selectivity is driven by serum adsorption and conformation on H- and O-terminated surfaces or by a direct effect of diamond surface dipoles on the cells. We also provide perspectives for potential bio-electronic applications.

## 2 MATERIALS AND METHODS

Diamond films are grown on (100) oriented silicon substrates (13 mm in diameter, 500  $\mu\text{m}$  thickness, RMS roughness of < 0.6 nm) by microwave plasma process using total gas pressure 50 mbar, substrate temperature 800°C, 1% CH<sub>4</sub> in H<sub>2</sub> and total power 2.5 kW. This process results in a growth of continuous, smooth and high quality nanocrystalline diamond film (Potocky, 2007; Kromka, 2008). X-ray photocurrent spectroscopy (XPS) detects that the films are 95% pure diamond (Zemek, 2006). The diamond film thickness is 300-400 nm. Average crystal size is 50 nm, RMS roughness at 1x1  $\mu\text{m}^2$  area is 15-20 nm as measured by AFM using standard silicon tips of nominal radius < 10 nm. The silicon substrates are coated with NCD film on both

sides, silicon is thus hermetically encapsulated in the diamond.

The diamond films were further chemically cleaned in acids (97.5% H<sub>2</sub>SO<sub>4</sub> + 99% powder KNO<sub>3</sub>) at 200°C for 30 minutes. The surface was then hydrogenated at 800°C for 10 minutes. NCD films were lithographically processed to generate alternating H- and O-terminated patterns of 30 to 200  $\mu\text{m}$  widths. A positive photoresist ma-P 1215 (micro resist technology GmbH, Germany) was applied. NCD films with lithography mask were treated in oxygen radio-frequency plasma (300W power, 3 minutes process time) to oxidize the surface and hence to generate the hydrophilic patterns. Then the sample was rinsed in a stripper, de-ionized water and dried. This process removed possible surface contamination (Rezek, 2006a). The H-/O-termination quality was proved by a scanning electron microscope (SEM; JEOL Superprobe 733). Electronic measurements detected a surface conductivity of 10<sup>-5</sup> S/sq on the H-terminated surfaces (Kozak, 2008). Surfaces with O-termination were highly resistive. The NCD samples were sterilized in 70% ethanol for 10 minutes prior to cell plating. The device concept is schematically shown in Figure 1.

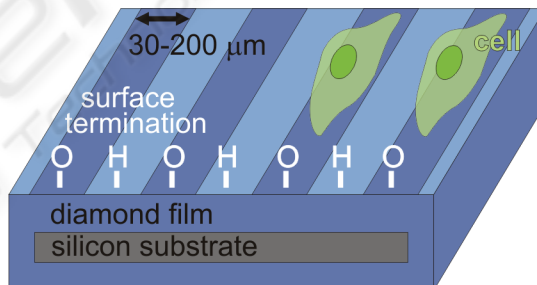


Figure 1: Schematic picture of silicon substrate hermetically coated with NCD layer with stripe-like patterns having hydrogen or oxygen surface termination. Cell adhesion on the O-terminated region is also schematically indicated.

SAOS-2 cells (human osteoblast-like cell line) (DSMZ GmbH), were grown in McCoy's 5A medium (BioConcept) supplemented with heat inactivated fetal bovine serum (FBS; Biowest) of various concentrations (0-15%), penicillin (20 U/ml) and streptomycin (20  $\mu\text{g}/\text{ml}$ ). Note that the SAOS-2 is a standard and well-defined cell line. Thus the results can be compared between various series of experiments as well as with reports in the literature. Cells were plated at the densities of 2,500 and 10,000 cells/cm<sup>2</sup> using a droplet technique: substrate surface was covered by 100  $\mu\text{l}$  droplet of cell

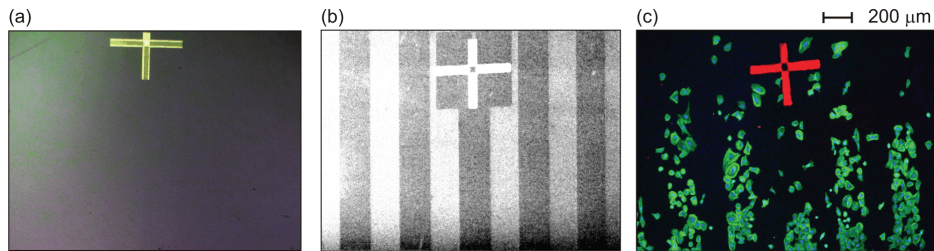


Figure 2: Nanocrystalline diamond film with 200 $\mu\text{m}$  wide H-/O-terminated patterns: (a) optical (bright field) image prior to cell plating showing optically transparent and featureless surface, (b) scanning electron microscopy image prior to cell plating where bright stripes correspond H-termination and dark stripes O-termination of the diamond surface due to their opposite electron affinity, (c) fluorescent microscopy image of osteoblastic cells cultivated on the substrate. The alignment cross is used for correlation of the surface termination micro-patterns with the cells.

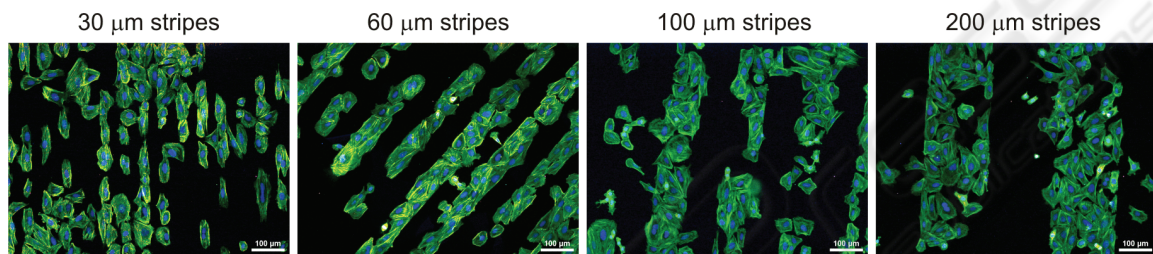


Figure 3: Fluorescent microscopy images of osteoblastic cells (SAOS-2) cultivated in McCoy's medium supplemented with 15% FBS for 2 days on H-/O-terminated stripes of different widths (30 $\mu\text{m}$ , 60 $\mu\text{m}$ , 100 $\mu\text{m}$  and 200 $\mu\text{m}$ ) on diamond films. Initial cell concentration was 2,500 cells/cm $^2$ . The fluorescence shows actin stress fibers (green) and nuclei (blue). Scale bar is 100 $\mu\text{m}$ .

suspension in the appropriately supplemented medium, let to incubate for 2 h (adhesion time), and then 1.4 ml of the medium was added. In case of 0% FBS, the cells were plated and incubated for 2 h in the medium without the serum. Then the 15% FBS-supplemented medium was added to facilitate further cell cultivation. After plating, the cells were cultivated for 48 hours in 5% CO<sub>2</sub> at 37°C.

An advantage of the applied droplet technique is a precise control of the applied number of cells on the sample. A disadvantage is slightly non-homogenous distribution of cells over the sample with lower concentration on the edge and higher concentration in the middle of the sample. Therefore, the microscopic images were taken from comparable areas on the samples.

Adhesion and morphology of SAOS-2 cells were characterized by fluorescent staining of actin stress fibers (phalloidin-Alexa 488 - 1:100, Molecular Probes) and nuclei (DAPI - 1:1000, Sigma) according to the protocol in Ref. (Kalbacova, 2007b). The staining was visualized using the E-400 epifluorescence microscope (Nikon); digital images were acquired with a DS-5M-U1 Color Digital Camera (Nikon).

As the adhesion and growth of osteoblastic cells is mediated by proteins, the adsorption, adhesion,

and conformation of FBS itself on the H- and O-terminated diamond was also investigated. Polished IIa (100) mono-crystalline diamonds were used as substrates to minimize the contribution from surface morphology of NCD films. The mono-crystalline diamond surface was H- or O-terminated using the same procedures as for NCD films. A droplet of 15% FBS in the McCoy's 5A medium was applied on the diamond substrates for 10 min. Then the whole samples were immersed in the fluid cell containing the same FBS/McCoy's medium and characterized by AFM (Ntegra, NTMDT).

AFM measurements were performed in the medium using doped silicon cantilevers (BSMulti75Al) with the typical force constant of 3 N/m, resonance frequency 75 kHz in air (30 kHz in the medium), and nominal tip radius <10 nm. Surface morphologies were investigated in oscillating-mode AFM (OM-AFM), where the tip-surface interaction is controlled by adjusting the AFM amplitude set-point ratio. Free oscillation amplitude of 60 nm and the set-point ratio of 50% were typically used. The parameters were optimized not to influence the soft FBS layer yet to provide optimal resolution and contrast. A nanoshaving procedure (Rezek, 2006b; Rezek, 2007a) was applied to evaluate the protein layer thickness. First,

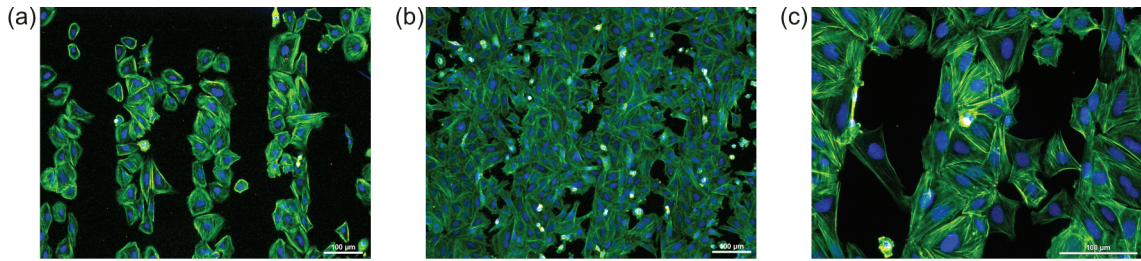


Figure 4: Fluorescent microscopy images of osteoblastic cells (SAOS-2) cultivated for 2 days on 100 $\mu\text{m}$  H-/O-terminated stripes on diamond films: (a) low initial cell seeding concentration (2,500 cells/cm $^2$ ), (b) high initial cell seeding concentration (10,000 cells/cm $^2$ ), and (c) cells bridging of unfavorable H-terminated regions. The fluorescence shows actin stress fibers (green) and nuclei (blue). Scale bar is 100 $\mu\text{m}$ .

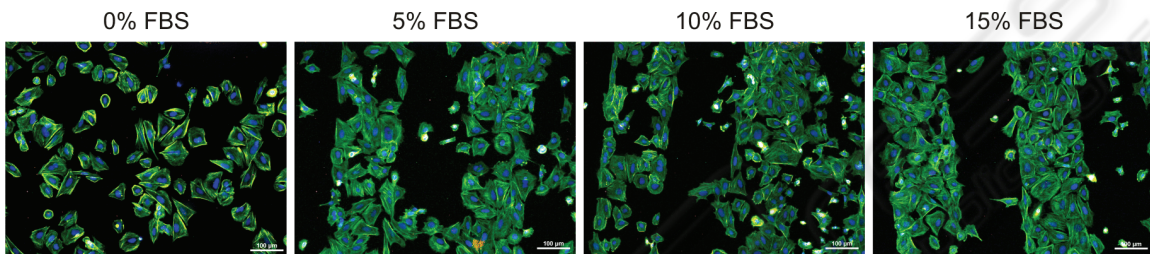


Figure 5: Fluorescent microscopy images of osteoblastic cells (SAOS-2) cultivated for 2 days on 200 $\mu\text{m}$  H-/O-terminated stripes on diamond films in McCoy's medium supplemented with different fetal bovine serum (FBS) concentrations (0, 5, 10, and 15%). Scale bar is 100 $\mu\text{m}$ .

a region of 2x2  $\mu\text{m}^2$  was scanned in contact AFM (C-AFM) and then re-measured across somewhat larger area by OM-AFM. The force applied during C-AFM was approx. 200 nN. The interaction forces in OM-AFM are orders of magnitude lower. The FBS layer thickness was then determined as the difference between average height values across 1  $\mu\text{m}^2$  of the FBS layer surface and 1  $\mu\text{m}^2$  of the nanoshaved area where FBS was removed. Several regions were probed on each sample to determine the error bar from root-mean-square (RMS) roughness values and statistical errors. Autocorrelation function of the images was calculated to determine typical lateral feature size ( $L_x$ ).

### 3 RESULTS

Correlation of oxygen- and hydrogen-terminated micro-patterns on the diamond films with patterns of cell adhesion on such structures is illustrated in Figure 2. Figure 2(a) shows a bright field image of the micro-structured sample in optical microscope before cell seeding. The surface is featureless as the patterns are optically invisible. Figure 2(b) presents SEM image of the sample, where H- and O-terminated patterns (width of 200  $\mu\text{m}$ ) are clearly

identified due to their different electronic properties. The bright stripes correspond to the H-terminated NCD surface, having negative electron affinity (Maier, 2001). The dark stripes represent the O-terminated NCD surface. Fluorescently stained human osteoblasts adherent on 200  $\mu\text{m}$  wide patterned surface are presented in Figure 2(c). By correlating a position of the alignment mark in SEM and fluorescent microscopy pictures, it is evident that the osteoblastic cells preferentially colonize the O-terminated (hydrophilic) patterns.

Figure 3 shows that the cells adhere preferentially onto O-terminated stripes independently of the stripe width in the range of 30–200 $\mu\text{m}$ . Two types of cell adhesion patterns are detectable. Cells on the narrow stripes (30 $\mu\text{m}$  – smaller than the cell size) are elongated and form cell-by-cell arrays. On wider stripes (60, 100, and 200 $\mu\text{m}$  – bigger than the cell size) the cells spread and fill the entire width of the stripe. At the micro-pattern borders they form a sharp boundary.

Osteoblast adhesion onto the NCD surface is affected by the initial cell seeding concentration. Figure 4 illustrates higher selectivity for cell adhesion on the O-terminated surface at lower initial cell seeding density (2,500 cells/cm $^2$ ). There is still some free space for cell spreading and expansion within the hydrophilic region. On the other hand, cells plated at the higher density (10,000 cells/cm $^2$ )

colonize not only hydrophilic areas but also unfavorable hydrophobic regions (Figure 4(b)). Figure 4(c) presents an abnormally long single cell (left image side) as well as clusters of several cells (right image side) that can bridge and colonize the hydrophobic area.

Figure 5 demonstrates the influence of different initial FBS concentrations (0, 5, 10, and 15%) in the culture medium on the cell attachment onto the H-/O-patterned surface. The range of serum concentrations 5-15% does not significantly affect the cell adhesion pattern. The cells follow the H-/O-terminated micro-patterns in the same way as shown in the previous figures. In a sharp contrast, cells plated in FBS-free medium colonize the surface independently of the micro-patterns. The cell selectivity is obviously determined by the FBS proteins.

Figure 6 shows OM-AFM topography image of the FBS layer on diamond with stripe-like patterns of hydrogen and oxygen surface terminations. The diagonal lines in the background are due to polishing of the diamond substrate. The roughness of diamond substrate is about 0.6 nm. On this background one can see clear stripes on the O-terminated surface. There are also some small scattered islands of similar thickness on the H-terminated stripes, most likely due to certain degree of non-specific adsorption. When the height of stripes is probed by the nanoshaving method, we find that the layer thickness of the layer adsorbed on O-terminated diamond is  $4 \pm 2$  nm. Even on H-terminated surface (outside of the islands) there is a thin layer of  $1.5 \pm 2$  nm. Hence the FBS layer is present on both types of diamond surfaces, although in the different thickness.

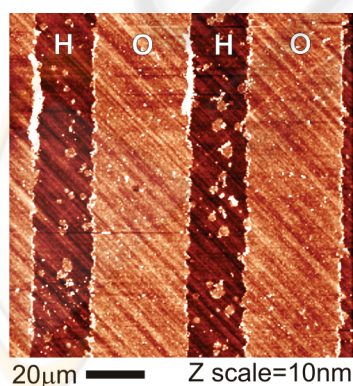


Figure 6: AFM topography image of a fetal bovine serum (FBS) layer on the diamond with stripe-like patterns of H and O surface terminations.

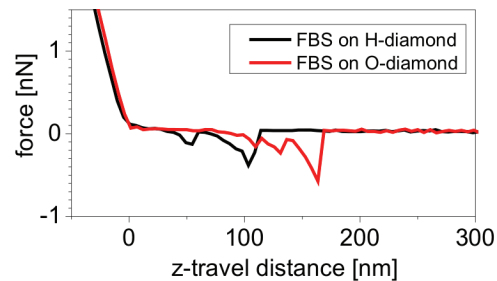


Figure 7: AFM force curves on H- and O-terminated diamond with the adsorbed FBS layer.

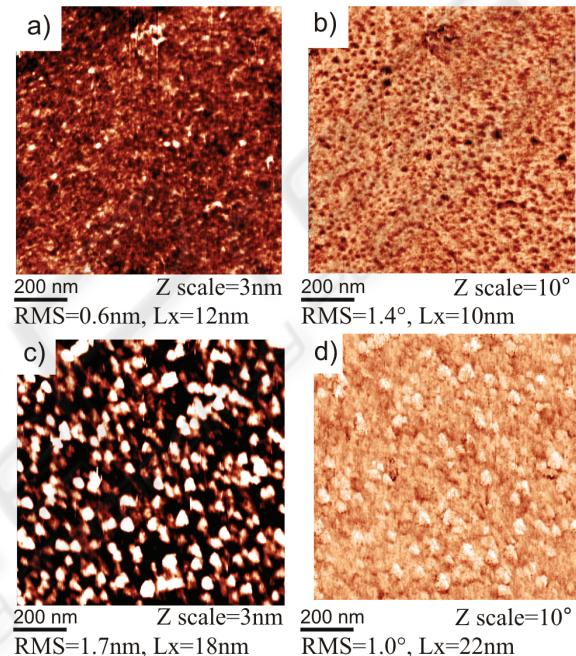


Figure 8: AFM measurements in FBS/McCoy's medium on hydrogen- and oxygen-terminated diamond surfaces with adsorbed FBS layers: topography and phase image on (a-b) FBS/H-terminated diamond (c-d) FBS/O-terminated diamond.

Figure 7 shows force curves obtained by force spectroscopy on H- and O-terminated diamond. The force curves exhibit  $500 \pm 100$  pN interaction between tip and surface on both H- and O-terminated diamond. Similar forces and shapes were found between cantilevers functionalized by bovine serum albumin and glass surfaces after deposition of proteins (Popov, 2007). Hence also the protein molecules from FBS are present on both H- and O-terminated diamond.

Figure 8 shows the detailed topography and phase images on both types of surfaces. Values of RMS roughness and lateral feature size (Lx) are also given. The roughness of FBS layer on O-terminated diamond (1.7 nm) is about two times higher

compared to H-terminated diamond (0.6 nm). The topographic features are different, with a kind of ridge-like shapes around valleys on H-terminated diamond and hillock-like shape on O-terminated diamond. Correspondingly, the feature size is also different, about 10 nm on H-terminated diamond and 20 nm on O-terminated diamond. A pronounced difference is detected also in the AFM phase images. AFM phase image of the adsorbed layer on H-terminated diamond is dominated by dark dots correlated with protrusions in morphology. On O-terminated diamond, brighter spots having darker boundaries are correlated with the hillocks.

## 4 DISCUSSION

In correlation with previous reports on homogeneous surface termination of diamond (Kalbacova, 2007a; Bacakova, 2007) we find that in case of H/O micro-patterns the cells colonize preferentially hydrophilic (O-terminated) stripes forming confluent arrays with sharp edges separating O- and H- terminated regions. The cells generally did not show any decreased viability, however some of them (preferentially on hydrophobic region) remain rounded for an extended period of time exhibiting poor cell-substratum-compatibility (Liu, 2007; Michalikova, 2008). Evolution of cell morphology on hydrophobic surfaces is slower, but otherwise not remarkably different than that observed for human osteoblasts (hFOB) (Liu, 2007) or SAOS-2 on more hydrophilic surfaces – it is an example of the time-cell-substratum-compatibility-superposition principle.

Also noteworthy is bridging of unfavorable H-terminated regions as illustrated in Figure 4(c). This is obviously enabled by connection to the cells on the O-terminated regions because solitaire cells on the H-terminated regions exhibit bad adhesion and reduced metabolic activity (Kalbacova, 2007a; Kalbacova, 2008). To reach the optimal status on unfitting surface, cells will communicate with each other, exchanging growth factors and various stimuli as well as produce extracellular matrix (ECM) and thus modify the surface with proteins and proteoglycans underneath to overcome the inhospitable environment. It is known that proteins adsorbed onto the substrate surface do not become permanently immobilized. They will be enzymatically degraded, denatured, they undergo conformational and configuration changes and will even be replaced by other proteins (Zeng, 1999). However, when more cells are able to gently attach

to hydrophobic surface in a specific pattern (forming a bridge between two hydrophilic stripes) then these cells may form ECM faster due to support from their proliferating neighbors, thus masking unsuitable properties of the surface. This may be very useful mechanism for bio-electronic applications as it enables to overgrow electrically conductive H-terminated surface when it is surrounded by O-terminated regions at small enough dimensions.

As the cell adsorption is protein mediated, a question arises whether the specific cell adsorption is due to direct effect of diamond surface dipoles on the cells or due to differences in protein adsorptions on the micro-patterns. Figure 5 clearly demonstrates that cells plated without protein (FBS-free medium) do not sense any chemical micro-patterning, whereas cells plated in FBS-supplemented medium clearly follow the hydrophilic patterns. It proves that the cell selectivity is driven by the FBS protein adsorption. Since protein adsorption is much more rapid than the transport of cells to the surface, it is expected that the interaction of host cells with the material is determined by the nature of this adsorbed protein layer.

AFM study of the protein layers revealed that FBS adsorbs on both types of diamond surfaces. This is in agreement with previous reports that albumin adsorbs on both hydrophilic and hydrophobic surfaces (Browne, 2004). Here, the adsorbed thickness differs by few nm. It should be noted that FBS layer is a soft matter so there is some uncertainty in determining its thickness by AFM because even in OM-AFM the height may be underestimated (Rezek, 2007a; Rezek, 2007b). Another influence on the observed step in the height across the nanoshaved region may be wear of the substrate material. As the flat bulk diamond is very hard compared to proteins and its wear is extremely low, only the FBS layer was penetrated and removed by the nanoshaving forces applied here.

The cell selectivity is thus not determined merely by FBS layer presence. More subtle differences must be considered for explaining the selective adsorption, such as protein denaturation on hydrophobic surfaces (Ukrainsev, 2007; Zeng, 1999). Detailed studies of surface morphology revealed clear differences in surface roughness, morphological features and phase images between the protein layers on H- and O-terminated diamond. By comparison with the literature (Browne, 2004), where similar difference in topography on polystyrene substrates were shown, the most important factor for the cell growth on diamond seems to be the wetting property of the surface

rather than any other specific property of the diamond films.

One has to critically consider that the actual composition of the adsorbed layers may be different on H- and O-terminated diamond because various proteins (albumin, fibronectin, vitronectin, etc.) from FBS may influence the cell adhesion in different ways. Further experiments are needed to elucidate these details.

## 5 CONCLUSIONS

Chemical patterning of diamond films by hydrogen and oxygen surface atoms enables self-assembly of human osteoblastic cell micro-arrays. The cell adhesion and assembly on diamond can be further controlled and optimized by biochemical factors. The cells strongly prefer O-terminated patterns. The best selectivity is achieved for lower initial cell concentrations (2,500 cells/cm<sup>2</sup>), regardless of surface geometry and commonly used protein (FBS) concentrations (5 to 15%). Widths of the patterns affect the shape of adhered cells in the following way: i) good cell spreading with a sharp boundary was observed on broader stripes and ii) elongated cell chains were observed on stripes which were narrower than the cell size. Higher initial concentration of cells enables colonization of less favorable H-terminated surface regions, which are electrically conductive and can be employed in electronic devices. A non-preferential cell adhesion is found when the initial cell adhesion occurs without the serum presence. Hence the cell selectivity is driven by the FBS properties on H- and O-terminated surfaces. AFM detected presence of the FBS layer on both types of surfaces. However, the layer thickness and microscopic morphology are rather different. This may be the reason for the cell selectivity. Further experiments are needed to elucidate details of the selectivity, such as particular composition of the adsorbed layers and so on.

Nevertheless, the presented data may already provide valuable information for application of diamond films in tissue engineering, implants, bio-electronics, and biotechnology in general. We speculate that similar cell behavior will occur also when using other cell lines.

## ACKNOWLEDGEMENTS

This work was supported by the Academy of Sciences of the Czech Republic contracts KAN400100701, AV0Z10100521, and Czech Ministry of Education, Youth and Sport projects LC-510 and MSM0021620806. The authors would like to express their thanks to Ing. Vlastimil Jurka, Zdena Poláčková, Dr. Zdeněk Potměšil (all Inst. Phys. ASCR) for a kind assistance with photolithography, and surface treatments, Jana Sovová (Inst. Inh. Met. Disorders, 1st Fac. Med., Charles Uni.) for technical assistance and Mgr. Veronika Barešová (Inst. Inh. Met. Disorders, 1st Fac. Med., Charles Uni.) for a kind assistance with fluorescent microscopy.

## REFERENCES

- Bacakova, L., Grausova, L., Vacik, J., Franczek A., Blazewicz, S., Kromka, A., Vanecek, M. & Svorcik, V. (2007). Improved adhesion and growth of human osteoblast-like MG 63 cells on biomaterials modified with carbon nanoparticles. *Diamond and Related Materials*, 16, 2133–2140.
- Bajaj, P., Akin, D., Gupta, A., Sherman, D., Shi, B., Auciello, O. & Bashir, R. (2007). Ultrananocrystalline diamond film as an optimal cell interface for biomedical applications. *Biomedical Microdevices*, 9, 787-794.
- Browne, M. M., Lubarsky, G. V., Davidson, M. R. & Bradley, R. H. (2004). Protein adsorption onto polystyrene surfaces studied by XPS and AFM. *Surface Science*, 553, 155–167.
- Garrido, A.J., Nebel, C. E., Todt, R., Roesel, G., Amann, M. -C. & Stutzmann, M. (2003). Fabrication of in-plane gate transistors on hydrogenated diamond surfaces. *Applied Physics Letters*, 82, 988-990.
- Kalbacova, M., Kalbac, M., Dunsch, L., Kromka, A., Vanecek, M., Rezek, B., Hempel, U. & Kmoch, S. (2007a). The effect of SWCNT and nano-diamond films on human osteoblast cells. *Physica status solidi (b)*, 244, 4356–4359.
- Kalbacova, M., Roessler, S., Hempel, U., Tsaryk, R., Peters, K., Scharnweber, D., Kirkpatrick, C. J., & Dieter, P. (2007b). The effect of electrochemically simulated titanium cathodic corrosion products on ROS production and metabolic activity of osteoblasts and monocytes/macrophages. *Biomaterials*, 28, 3263–3272.
- Kalbacova, M., Michalikova, L., Baresova, V., Kromka, A., Rezek, B. & Kmoch, S. (2008). Adhesion of osteoblasts on chemically patterned nanocrystalline diamonds. In press in *Physica status solidi (b)*.
- Kozak, H., Kromka, A., & Rezek, B. (2008). Enhancing nanocrystalline diamond surface conductivity by deposition temperature and chemical post-processing. Submitted in *Physica status solidi (a)*.

- Kromka, A., Rezek, B., Remes, Z., Michalka, M., Ledinsky, M., Zemek, J., Potmesil, J. & Vanecek, M. (2008). Formation of continuous nanocrystalline diamond layer on glass and silicon at low temperatures. In press in *Chemical Vapor Deposition*.
- Liu, X., Lim, J. Y. F., Donahue, H. J., Dhurjati, R., Mastro, A. M. & Vogler, E. A. (2007). Influence of substratum surface chemistry/energy and topography on the human fetal osteoblastic cell line hFOB 1.19: Phenotypic and genotypic responses observed in vitro. *Biomaterials*, 28, 4535–4550.
- Maier, F., Ristein, J. & Ley, L. (2001). Electron affinity of plasma-hydrogenated and chemically oxidized diamond (100) surfaces. *Physical Review B*, 64, 165411.
- Michalikova, L., Rezek, B., Kromka, A., Kozak, H., Grausova, L., Bacakova, L., Vanecek, M., Kocka, J. & Kalbacova, M. (2008). Selective Adhesion and Arrangement of osteoblast-like cells on hydrophilic and hydrophobic nanocrystalline diamond micro-patterns. Submitted to *Thin Solid Films*.
- Nebel, C. E. (2003). From gemstone to semiconductor. *Nature Materials*, 2, 431-432.
- Popov, C., Kulisch, W., Reithmaier, J., Dostalova, T., Jelinek, M., Anspach, N. & Hammann, C. (2007). Bioproperties of nanocrystalline diamond/amorphous carbon composite films. *Diamond and Related Materials*, 16, 735-739.
- Potocky, S., Kromka, A., Potmesil, J., Remes, Z., Vorlicek, V., Vanecek, M., & Michalka, M. (2007). Investigation of nanocrystalline diamond films grown on silicon and glass at substrate temperature below 400°C. *Diamond and Related Materials*, 16, 744-747.
- Rezek, B., & Nebel, C. E. (2006a). Electronic properties of plasma hydrogenated diamond surfaces: A microscopic study. *Diamond and Related Materials*, 15, 1374–1377.
- Rezek, B., Shin, D., Nakamura, T. & Nebel, C. E. (2006b). Geometric properties of covalently bonded DNA on single-crystalline diamond. *Journal of American Chemical Society*, 128, 3884-3885.
- Rezek, B., Shin, D., Uetsuka, H. & Nebel, C. E. (2007a). Microscopic diagnostics of DNA molecules on monocrystalline diamond. *Physica status solidi (a)*, 204, 2888-2897.
- Rezek, B., Shin, D. & Nebel, C. E. (2007b). Properties of hybridized DNA arrays on single-crystalline undoped and boron-doped (100) diamonds studied by atomic force microscopy in electrolytes. *Langmuir*, 23, 7626-7633.
- Rezek, B., Shin, D., Watanabe, H. & Nebel, C. E. (2007c). Intrinsic hydrogen-terminated diamond as ion-sensitive field effect transistor. *Sensors and Actuators B*, 122, 596-599.
- Shakenraad, J. M., & Busscher, H. J. (1989). Cell-polymer interactions:the influence of protein adsorption. *Colloids and Surfaces*, 42, 331–343.
- Song, K. S., Hiraki, T., Umezawa, H. & Kawarada, H. (2007). Miniaturized diamond field-effect transistors for application in biosensors in electrolyte solution. *Applied Physics Letters*, 90, 063901.
- Tachiki, M., Kaibara, Y., Sumikawa, Y., Shigeno, M., Banno, T., Song K. S., Umezawa, H. & Kawarada, H. (2003). Diamond nanofabrication and characterization for biosensing application. *Physica status solidi (a)*, 199, 39-43.
- Tang, L., Tsai, C., Gerberich, W. W., Kruckeberg, L. & Kania, D. R. (1995). Biocompatibility of chemical-vapour-deposited diamond. *Biomaterials*, 16, 483-488.
- Ukrainstev, E. V., Kiselev, G. A., Kudrinskii, A. A., Lisichkin, G. V. & Yaminskii, I. V. (2007). Formation of lysozyme fibrils on a solid support. *Polymer Science*, 49, 6-9.
- Yang, W., Auciello, O., Butler, J. E., Cai, W., Carlisle, J. A., Gerbi, J. E., Gruen, D. M., Knickerbocker, T., Lasseter, T. L., Russell, J. N. Jr., Smith, L. M. & Hamers, R. J. (2002). DNA-modified nanocrystalline diamond thin-films as stable, biologically active substrates. *Nature Materials*, 1, 253-257.
- Yang, W., Butler, J. E., Russell, J. N. & Hamers, R. J. (2004). Interfacial electrical properties of DNA-modified diamond thin films: Intrinsic response and hybridization-induced field effects. *Langmuir*, 20, 6778-6787.
- Zemek, J., Houdkova, J., Lesiak, B., Jablonski, A., Potmesil, J., & Vanecek, M. (2006). Electron spectroscopy of nanocrystalline diamond surfaces. *Journal of Optoelectronics and Advanced Materials*, 8, 2133–2138.
- Zeng, H., Chittur, K. K. & Lacefield, W. R. (1999). Analysis of bovine serum albumin adsorption on calcium phosphate and titanium surfaces. *Biomaterials*, 20, 377–384.